Promotion of binding of von Willebrand factor to platelet glycoprotein Ib by dimers of ristocetin

Marc F. HOYLAERTS, Katarine NUYTS, Kathelijne PEERLINCK, Hans DECKMYN and Jozef VERMYLEN
Center for Molecular and Vascular Biology, University of Leuven, Leuven, Belgium

In the absence of high shear forces, the *in vitro* binding of human von Willebrand factor (vWF) to its platelet receptor glycoprotein Ib (GPIb) can be promoted by two well-characterized mediators, botrocetin and ristocetin. Using purified vWF and GPIb, we have investigated the mechanism by which ristocetin mediates this binding. Specific binding of vWF monomers to GPIb occurred with a 1:1 stoichiometry, but high-affinity binding required the participation of two ristocetin dimers. Binding was strongly dependent on pH and inhibited by low poly-L-lysine concentrations, indicating ristocetin-dependent charge neutralization during the interaction. With increasing ristocetin concentrations, vWF binding depended progressively less on the involvement of its A1 loop, which is compatible with a model in which the two ristocetin dimers bridge the vWF–GPIb complex on secondary sites. In agreement with this model, the ristocetin-dimer-promoted stabilization of vWF on GPIb was abolished by low concentrations of poly(Pro-Gly-Pro), which is known to complex ristocetin dimers. Mechanistic analysis of the inhibition of vWF binding by the recombinant vWF fragment Leu^{504}–Ser^{728} (VCL), which covers the entire A1 loop, revealed an affinity of VCL for GPIb comparable with that of the botrocetin–vWF complex for GPIb, and identified a specific but 20-fold lower affinity of VCL in the presence of ristocetin. The proline-rich peptides flanking the vWF A1 loop, Cys^{474}–Val^{489} and Leu^{694}–Asp^{709}, inhibited vWF binding semispecifically by competitively interfering with the formation of the GPIb–vWF complex rather than by complexation of free ristocetin dimers. In conclusion, ristocetin-promoted binding of vWF to its GPIb receptor results from charge neutralization and interactions involving proline residues in the vicinity of the natural interaction sites present on both GPIb and the A1 domain of vWF.

INTRODUCTION

von Willebrand factor (vWF) is a multimeric plasma protein that mediates the adhesion of platelets to vascular subendothelium exposed to flowing blood as a consequence of tissue damage (Ruggeri and Ware, 1992). During this phenomenon exposed vessel-wall extracellular matrix collagens interact with circulating vWF; this binding is mediated by specific amino acid sequences located in the functional A1 and A3 vWF domains (Pareti et al., 1987; Kalafatis et al., 1987). Subsequently, at sufficiently elevated shear forces, collagen-bound vWF interacts with the glycoprotein Ib (GPIb) receptor located on circulating platelets via sequences close to or located within the vWF A1 loop, which itself is shaped by a disulphide bridge between the cysteine residues 509 and 695 (Meyer and Girma, 1993).

It is believed that high shear forces induce a conformational change in the vessel-wall-associated vWF, accompanied by exposure of the platelet GPIb-binding site (Bolhuis et al., 1981). Under *in vitro* conditions of low shear forces, this binding can be simulated by two non-physiological mediators, ristocetin and botrocetin (Coller, 1985). Ristocetin is a glycopeptide antibiotic, synthesized by the actinomycete *Nocardia lurida*, that spontaneously dimerizes with an equilibrium constant around 1.1 mg/ml (Waltho and Williams, 1989). The flocculation of fibrinogen and agglutination of platelets observed in the presence of ristocetin are believed to be the result of cross-linking induced by ristocetin dimers that bridge proline-rich β-turns in separate protein molecules (Scott et al., 1991). Two-chain botrocetin on the other hand, a 32 kDa protein isolated from the venom of the snake *Bothrops jararaca*, forms a soluble complex with vWF (Fujimura et al., 1991). In addition, although quite a large number of anti-vWF monoclonal antibodies have been reported to block ristocetin-induced platelet aggregation by inhibition of vWF binding to GPIb (Fujimura et al., 1992), we have recently described an anti-vWF monoclonal antibody, 1C1E7, that is capable of positively modulating the interaction of vWF with GPIb, i.e. by lowering the ristocetin requirements during ristocetin-induced platelet aggregation (Tornai et al., 1993).

Three vWF sequences are at present believed to be involved in the binding of vWF to GPIb: two non-contiguous sequences Cys^{474}–Pro^{488} and Leu^{694}–Pro^{708} (Mohri et al., 1988, 1989), which flank the A1 loop, and a third sequence (Asp^{514}–Glu^{542}), which resides inside the A1 loop (Berndt et al., 1992). Because the synthetic peptide Asp^{514}–Glu^{542} inhibits ristocetin-independent binding of both asialo-vWF and bovine vWF to GPIb, this sequence is thought to constitute a major part of the GPIb-binding site on vWF (Berndt et al., 1992). This hypothesis is further supported by the finding that three discontinuous sequences within the A1 loop located between Asp^{539} and Cys^{643} are involved in complex-formation of vWF with botrocetin (Sugimoto et al., 1991). In contrast with the well-understood mechanism underlying botrocetin-mediated vWF binding, the exact mechanism by which ristocetin mediates vWF binding to GPIb remains to be elucidated. The finding that the polyanionic aurin tricarboxylic acid (ATA) binds to the botrocetin interaction site in the A1 loop, and not only competes with botrocetin-mediated vWF binding to GPIb but also ristocetin-mediated binding, also points to the importance of the A1 loop in ristocetin-mediated vWF binding to GPIb (Girma et al., 1992). The observation that a vWF proteolytic fragment III-T2, which almost completely lacks the A1 loop, can still compete with ristocetin-dependent binding of native vWF as well as asialo-vWF to GPIb (Mohri et al., 1989) suggests that the sequences that flank the A1 loop contribute also to the binding to GPIb.

Abbreviations used: vWF, von Willebrand factor; GPIb, glycoprotein Ib; VCL, recombinant vWF fragment Leu^{504}–Ser^{728}; ATA, aurin tricarboxylic acid.

In view of the diagnostic use of ristocetin in the identification of patients with von Willebrand disease types I and II (Light et al., 1987), we mechanistically analysed how ristocetin mediates the binding of vWF to GPIb. For this purpose, vWF and GPIb were purified and their interactions studied by e.l.i.s.a. in the presence of the mediators, ristocetin and botrocetin and the modulating antibody 1C1E7. In order to delineate further contributions of the A1 loop during ristocetin-mediated vWF–GPIb interactions, inhibition of vWF binding was studied in the presence of the recombinant monomeric vWF fragment Leu^{504}–Ser^{728} (VCL) (Gralnick et al., 1992), ATA, the vWF peptides Cys^{474}–Val^{489} and Leu^{694}–Asp^{709}, poly-L-lysine and poly(Pro-Gly-Pro). The use of these well-defined inhibitors has enabled us to validate experimentally the proposed mechanism for ristocetin-promoted binding of vWF to GPIb.

MATERIALS AND METHODS

Purification of GPIb

Isolated platelets were successively frozen in the presence of 1 mM EDTA and thawed three times and pelleted at 24000 *g* (17000 rev./min). On solubilization of the pellet in 10 mM Tris/HCl buffer, pH 7.4, containing 1 mM EDTA and 10 mM CHAPS (Sigma, St. Louis, MO, U.S.A.) followed by centrifugation, the supernatant was loaded on a column of CNBr-conjugated AP-1 Sepharose; the anti-GPIb monoclonal antibody AP-1 used for this conjugation was generously provided by Dr. Kunicki, Scripps Research Institute, La Jolla, CA, U.S.A. On loading, this affinity column was washed with 10 mM Hepes buffer, pH 7.5, containing 1 mM EDTA and 2 mM CHAPS. The GPIb was isolated by elution with 2 M KSCN added to the wash buffer, and after dialysis it was stored at −80 °C. When tested by SDS/PAGE (Laemmli, 1970), the eluted and reduced proteins displayed three bands characteristic of both GPIb chains and the associated GPIX band, in addition to traces of bands corresponding to glycocalicin.

Purification of vWF

vWF was purified from human plasma cryoprecipitate by reprecipitation and bentonite-mediated fibrinogen depletion, followed by gel filtration on a Sepharose 4B-CL column (2.6 cm × 95 cm) (Ruggeri et al., 1992). On reduced SDS/polyacrylamide gels, over 90 % of the isolated protein appeared as a single 250 kDa band. Unless indicated, all experiments were carried out with a single preparation, selected because of its low degree of non-specific binding during e.l.i.s.a. (see below). On collection of the gel-filtration eluate into three fractions of decreasing molecular mass, vWF entities of progressively diminishing degree of multimerization were collected. Asialo-vWF was prepared from purified vWF by digestion with 0.2 unit of *Clostridium perfringens* neuraminidase (Sigma)/mg of vWF for 3 h at 37 °C, after which the neuraminidase was removed by gel filtration on the Sepharose 4B-Cl column.

Studies of interaction between vWF and GPIb

The interaction between purified vWF and GPIb was studied in an e.l.i.s.a. configuration. Purified GPIb was coated on the wells of microtitre plates at 2 μg/ml (200 μl/well) for 48 h at 4 °C in 10 mM Tris/HCl, pH 7.5, containing 10 mM NaCl and 10 mM NaN_3. After blocking of non-adsorbed sites with BSA (10 mg/ml), vWF (0–50 μg/ml) was incubated in the plates with ristocetin (0–2 mg/ml; Paesel-Lorei, Frankfurt, Germany) or botrocetin (0–1 μg/ml; Pentapharm LTI, Basel, Switzerland), in some experiments supplied with the home-made anti-vWF antibody 1C1E7 (0–50 μg/ml) to positively modulate binding of vWF (Tornai et al., 1993). Protein mixtures were pipetted into the microtitre-plate wells before the addition of ristocetin or botrocetin. All dilutions were made in PBS containing 0.1 % BSA and 0.002 % Tween 80. Control incubations were performed in the presence of identical concentrations of an irrelevant monoclonal antibody 7C7B3. In order to distinguish between specific, i.e. GPIb-dependent, and non-specific binding, GPIb-coated plates were presaturated with AP-1, which, when bound to the N-terminal loop of GPIb, specifically prevents binding of vWF (Montgomery et al., 1983). To study further the specificity of the binding and to analyse mechanistically the contribution of various vWF domains in the interaction with GPIb, botrocetin- and ristocetin-mediated vWF binding were studied in the presence of potential inhibitors such as the polymers (all obtained from Sigma) poly(Pro-Gly-Pro) (5.4 kDa; 0–10 μM), poly-L-lysine (3.97 kDa; 0–100 μM) and ATA (0.473 kDa; 0–3 μM). In addition, competitive-inhibition experiments were performed with the vWF fragment Leu^{504}–Ser^{728} (VCL; 0–80 nM), a recombinant disulphide-linked vWF fragment comprising the entire A1 loop, and one of the A1 flanking peptides (Leu^{694}–Pro^{708}) postulated to be involved in ristocetin-mediated vWF binding to GPIb. The VCL fragment was a gift from Dr. Garfinkel, Bio-Technology General, Rehovot, Israel. Finally, inhibition of binding by the vWF peptides Cys^{474}–Val^{489} and Leu^{694}–Asp^{709} was studied; both these peptides, which represent sequences flanking the A1 loop, were custom-synthesized and purified to homogeneity by h.p.l.c.

During e.l.i.s.a., GPIb-associated vWF was revealed by horseradish peroxidase-conjugated anti-vWF monoclonal antibodies 82D6A3 and 82D1E1 previously described for e.l.i.s.a.-based measurement of plasma vWF levels (Tornai et al., 1991).

Flocculation

Agglutination of vWF multimers of various size (75 μg/ml) by ristocetin (1.6 mg/ml) was studied in a Pye–Unicam SP 1800 spectrophotometer, by continuously recording the light-scattering signal at 600 nm, in the absence or presence of antibody 1C1E7 (50 μg/ml) or poly(Pro-Gly-Pro) (100 μM).

Mathematical analysis

Botrocetin (B)-mediated binding of vWF to GPIb can be represented by Scheme 1.

$$\begin{array}{ccc} & \overset{K_{A1}}{\rightleftharpoons} & \\ \text{GPIb+vWF–B} & & \text{GPIb–vWF–B} \\ \downarrow\uparrow K_B & & \\ \text{vWF} & & \\ + & & \\ \text{B} & & \end{array}$$

Scheme 1

The e.l.i.s.a. signal measured at 492 nm (A) is directly proportional to [GPIb–vWF–B] via an undefined staining constant (k) which, in addition to the amount of bound vWF, depends on the substrate concentration and the staining time:

$$A = k[\text{GPIb–vWF–B}] = \frac{k[\text{GPIb}][\text{vWF–B}]}{K_{A1}} \quad (1)$$

The total GPIb concentration can be obtained using the following expression:

$$[\text{GPIb}]^0 = [\text{GPIb}](1 + [\text{vWF–B}]/K_{A1})$$

which on substitution into eqn. (1) yields:

$$A = \frac{k[\text{GPIb}]^0}{1 + \dfrac{K_{a1}}{[\text{vWF–B}]}} \quad (2)$$

Double-reciprocal plots of A versus $[B]^0$ (for extrapolated infinite $[vWF]^0$ where [vWF–B] equals $[B]^0$) or of A versus $[VWF]^0$ (for extrapolated infinite $[B]^0$ where [VWF–B] equals $[vWF]^0$) thus allow determination of K_{A1}. As the actual concentrations of vWF bound to GPIb are of the order of ng/ml, we can neglect the fraction of vWF bound to GPIb in comparison with the sum of [vWF] and [vWF–B], i.e. $[vWF]^0 \approx [vWF] + [vWF–B]$. Similarly we can assume that $[B]^0 \approx [B] + vWF–B]$.

Substituting these relationships in the expression:

$$K_B = [vWF][B]/[vWF–B]$$

it is possible to calculate K_B from the total concentrations of vWF and botrocetin, and from [vWF–B], the latter derived from eqn. (1), in which k[GPIb–vWF–B] equals A and k[GPIb] equals $(A_{plateau} - A)$, $A_{plateau}$ itself being obtained from the double-reciprocal plots of A versus $[B]^0$ or $[vWF]^0$.

Inhibition of botrocetin-mediated vWF binding by the VCL fragment is represented in Scheme 2 and can be described by the following expression for the e.l.i.s.a. signal:

$$A = \frac{k[\text{GPIb}]^0}{1 + \dfrac{K_{A1}K_B}{[B][vWF]}\left(1 + \dfrac{[VCL]^0}{K_{VCL}}\right)} \quad (3)$$

yielding an intersection in plots of $1/A$ versus $[VCL]^0$ at $[VCL]^0 = -K_{VCL}$.

Ristocetin (R)-mediated binding of vWF to GPIb is controlled by two ristocetin dimes (RR) and can be represented by Scheme 3. A complex can form between GPIb and vWF on condition

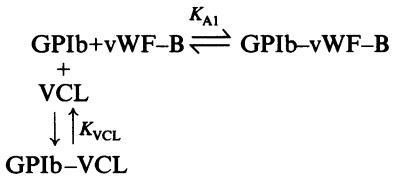

Scheme 2

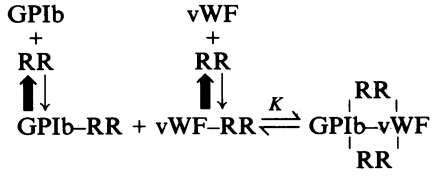

Scheme 3

that two ristocetin dimer bridges stabilize the interaction between the two proteins. No stable intermediates are formed between GPIb or vWF and the ristocetin dimers, i.e. [GPIb–RR] and [vWF–RR] are negligible. Therefore binding can be described by the following equation:

$$A = k\left[\begin{matrix}\text{RR}\\ \text{GPIb–vWF}\\ \text{RR}\end{matrix}\right] = \frac{k[\text{GPIb}][\text{RR}]^2[\text{vWF}]}{K} \quad (4)$$

in which K would be a third-order equilibrium constant. Whereas in this model $[vWF] = [vWF]^0$, the concentrations of R and RR are defined by the dimerization equilibrium constant $K_{eq.} = [R]^2/[RR] = 1.1$ mg/ml (Waltho and Williams, 1989). As A_{492} equals $k[\text{GPIb} = \text{RR}_2 = \text{vWF}]$ and $(A_{plateau} - A)$ equals k[GPIb], logarithmic transformation of eqn. (4) yields the following Hill plot:

$$\log A/(A_{plateau} - A) = 2\log[\text{RR}] + \log[\text{vWF}]^0 - \log K$$

Furthermore, as $[\text{GPIb}]^0 = [\text{GPIb}]\{1 + ([\text{RR}]^2[\text{vWF}]^0/K)\}$, quaternary complex-formation is described by the following equation:

$$A = \frac{k[\text{GPIb}]^0}{1 + \dfrac{K}{[\text{RR}]^2[\text{vWF}]^0}} \quad (5)$$

Plots of $1/A$ against $1/[vWF]^0$ are expected to be linear and to depend on the second power of the actual ristocetin dimer concentration, calculated from $[R]^0$ and $K_{eq.}$. Furthermore, both $1/A$ versus $1/[vWF]^0$ plots (constructed for various ristocetin concentrations) and $1/A$ versus $1/[RR]^2$ (constructed for various vWF concentrations) are predicted to intersect on the y-axis at $A = k[\text{GPIb}]^0$.

The specific inhibition of ristocetin-induced binding of vWF to GPIb by VCL can be represented by a model in which VCL binding to GPIb competes with binding of vWF to GPIb (Scheme 4). This can be described by the following equation:

$$A = \frac{k[\text{GPIb}]^0}{1 + \dfrac{K}{[\text{RR}]^2[\text{vWF}]^0}\left(1 + \dfrac{[VCL]^0}{K'_{VCL}}\right)} \quad (6)$$

Thus plots of $1/A$ versus $[VCL]^0$ will be linear for given concentrations of vWF and ristocetin. The slopes of these lines are inversely proportional to $[RR]^2$ and $[vWF]^0$. Plots constructed for various ristocetin (or vWF) concentrations but at constant vWF (or ristocetin) concentrations will intersect at $[VCL]^0 = -K'_{VCL}$.

Finally, the semispecific inhibition of ristocetin-induced vWF binding to GPIb by proline-rich peptides (P) such as Cys^{474}–Val^{489} and Leu^{694}–Asp^{709} can be represented as being the result of

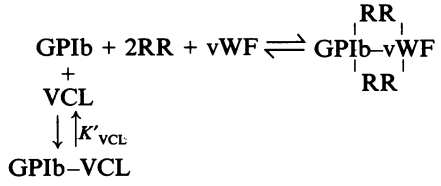

Scheme 4

$$\begin{array}{ccccc} \text{GPIb–P} & \overset{K_P}{\rightleftharpoons} & \text{P} + \text{GPIb} + 2\text{RR} + \text{vWF} & \rightleftharpoons & \begin{matrix}\text{RR}\\ |\\ \text{GPIb–vWF}\\ |\\ \text{RR}\end{matrix} \\ + & & + & & \\ \text{VCL} & & \text{VCL} & & \\ \downarrow\uparrow K'_{VCL} & & \downarrow\uparrow K'_{VCL} & & \\ \text{P–GPIb–VCL} & \rightleftharpoons & \text{P} + \text{GPIb–VCL} & & \end{array}$$

K_P

Scheme 5

peptide binding to GPIb during the ristocetin-mediated formation of the quaternary complex. Formally these peptides can be considered as competitive inhibitors because they prevent vWF binding to GPIb, or the inhibition by these peptides can be represented as follows:

$$A = \frac{k[\text{GPIb}]^0}{1 + \frac{K}{[\text{RR}]^2[\text{vWF}]^0}\left(1 + \frac{[\text{P}]^0}{K_P}\right)} \quad (7)$$

This expression is analogous to that describing the inhibition by VCL. To confirm finally that VCL- and peptide-binding sites were different, co-inhibition studies were performed, by varying $[\text{VCL}]^0$ versus $[\text{P}]^0$ at a constant concentration of vWF and ristocetin. This inhibition can be described by Scheme 5 and described by the following equation:

$$A = \frac{k[\text{GPIb}]^0}{1 + \frac{K}{[\text{RR}]^2[\text{vWF}]^0}\left(1 + \frac{[\text{P}]^0}{K_P}\right)\left(1 + \frac{[\text{VCL}]^0}{K'_{VCL}}\right)} \quad (8)$$

Only if VCL and the peptide target different sites with formation of the P–GPIb–VCL intermediate will an intersection be found in $1/A$ versus $[\text{VCL}]^0$ plots. When VCL and the peptides compete with vWF for the same site on GPIb, parallel lines are expected in reciprocal plots of A versus $[\text{VCL}]^0$, as the slope of the lines are no longer dependent on $[\text{P}]^0$.

Hill plots and double-reciprocal plots were graphically fitted to the data points by linear regression, and slopes and intercepts (±standard error) were calculated.

RESULTS

Botrocetin-mediated vWF binding to GPIb

Incubation of increasing concentrations of botrocetin with different vWF concentrations in freshly GPIb-coated microtitre plates resulted in dose-dependent binding of the progressively formed vWF–botrocetin complex (Figure 1a). Mathematical analysis of this binding according to Scheme 1 and eqn. (2) identified linear double-reciprocal plots of A versus $[\text{vWF}]^0$ (Figure 1b) or A versus $[\text{B}]^0$ (not shown). At infinite $[\text{vWF}]^0$, [vWF–B] equals $[\text{B}]^0$, hence replots of the y-intercepts from Figure 1(b) allow determination of K_{A1}. As shown in Figure 1(c), this replot was linear, yielding a value for K_{A1} of 0.25±0.09 nM. Similarly, a replot of the y-intercepts of the $1/A$ versus $1/[\text{B}]^0$ plot yielded a straight line with $K_{A1} = 0.32 \pm 0.11$ nM, severalfold lower than the value of 7 nM reported for botrocetin-mediated binding of vWF to the recombinant GPIb fragment identified as the vWF-binding domain (Murata et al., 1991). Calculation of the numerical value for K_B as outlined in the Materials and methods section revealed an equally high affinity for the vWF–botrocetin interaction ($K_B = 0.28 \pm 0.06$ nM). Comparable K_B values were calculated under conditions of low and high binding, confirming that the quantity of vWF bound to GPIb was negligible compared with the sum of free and botrocetin-complexed vWF.

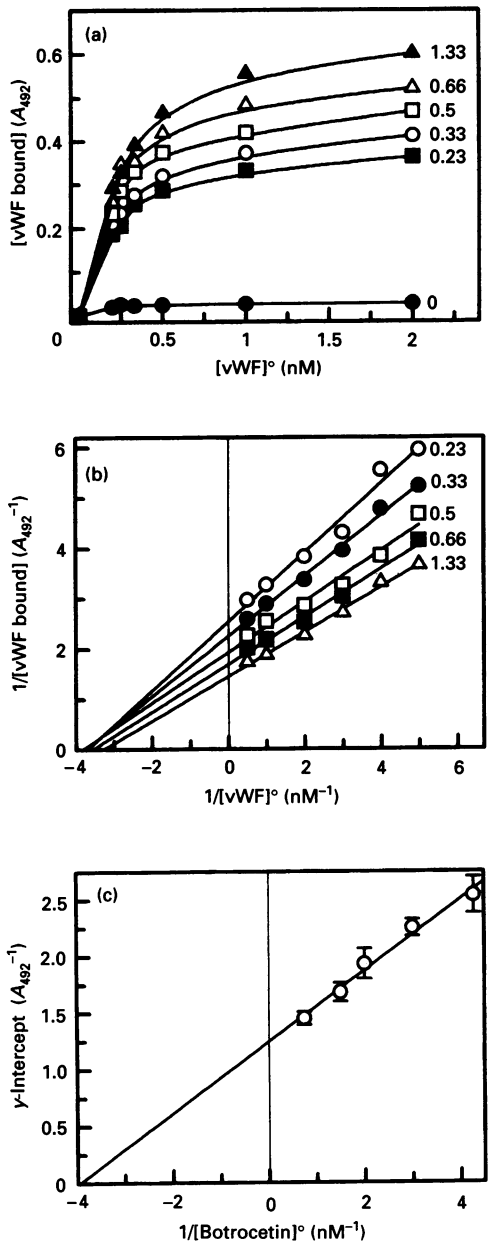

Figure 1 Mechanistic analysis of botrocetin-mediated vWF binding to GPIb

(**a**) Botrocetin-mediated binding of increasing vWF concentrations to GPIb-coated microtitre plates at the indicated botrocetin concentrations (0.23–1.33 nM); bound vWF was detected by a horseradish peroxidase-labelled anti-vWF monoclonal antibody. (**b**) Double-reciprocal plots of A versus $[\text{vWF}]^0$ for the binding of vWF to GPIb-coated microtitre plates at the indicated botrocetin concentrations (0.23–1.33 nM). (**c**) Replot of y-axis intercepts (±standard error) from (**b**) versus $1/[\text{B}]^0$.

To validate further the usefulness of GPIb directly coated on to a synthetic surface for the mechanistic study of the GPIb–vWF interaction, botrocetin-mediated vWF-binding studies were also carried out in the presence of increasing concentrations of the vWF fragment known as VCL, which because of the presence of

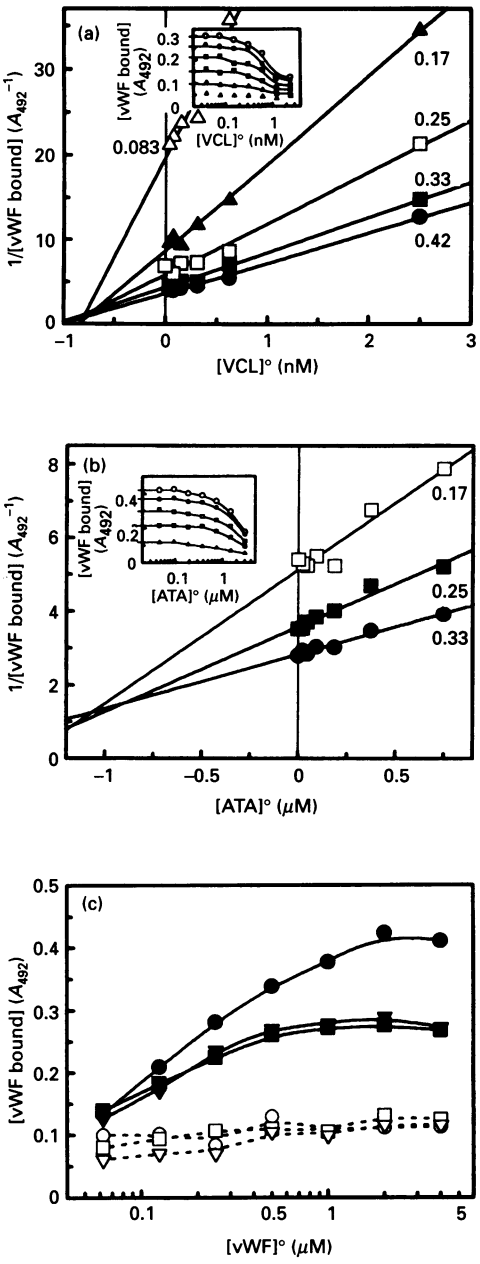

Figure 2 Specificity of botrocetin-mediated vWF binding

(**a**) Plots of $1/A$ versus $[VCL]^0$ during inhibition of the botrocetin-mediated binding of vWF (4 nM) to GPIb-coated microtitre plates, at the indicated botrocetin concentrations (0.083–0.42 nM). Inset: dose-dependent inhibition of botrocetin (0.042–0.42 nM)-mediated vWF (4 nM) binding by VCL (0–2.5 nM). (**b**) Plots of $1/A$ versus $[ATA]^0$ during inhibition of botrocetin-mediated binding of vWF (4 nM) to GPIb-coated microtitre plates, at the indicated botrocetin concentrations (0.17–0.33 nM). Inset: dose-dependent inhibition of botrocetin (0.042–0.42 nM)-mediated vWF (4 nM) binding by ATA (0–3 μM). (**c**) Botrocetin (0.2 nM)-mediated binding of increasing vWF concentrations (0–4 nM) to GPIb-coated microtitre plates, in buffer (■), and in the presence of 50 μg/ml anti-vWF antibody 1C1E7 (●) or a control antibody 7C7B3 (▼). The open symbols represent residual vWF binding to microtitre plates pretreated with the anti-GPIb antibody AP-1 at 10 μg/ml.

the critical A1 loop Cys^{509}–Cys^{695} disulphide bridge of vWF was reported to block vWF binding to GPIb effectively with an IC_{50} of 22 nM (Gralnick et al., 1992). As shown in the inset of Figure 2(a), for various concentrations of botrocetin, the VCL fragment strongly competes with botrocetin-mediated vWF binding to the coated GPIb. Mathematical analysis of this inhibition according to Scheme 2 and eqn. (3) identified linear plots of $1/A$ versus $[VCL]^0$ (Figure 2a), compatible with a competition between VCL and the botrocetin–vWF complex for binding to GPIb. The strength of this inhibition ($K_{VCL} = 0.8 \pm 0.2$ nM) reflects an affinity of VCL for GPIb only about 3-fold lower than that of the botrocetin–vWF complex itself, confirming that VCL is structurally comparable with the botrocetin-exposed A1 loop in vWF. Likewise, the inhibition of botrocetin-mediated vWF binding by ATA, which inhibits binding of vWF to GPIb as a consequence of its interaction with the vWF A1 loop, is dose-dependent (Figure 2b, inset). Mechanistic analysis of this inhibition (Figure 2b) identified an apparent inhibition constant $K_i = 1.1 \pm 0.2$ μM for the ATA–vWF interaction, a value reflecting an even higher affinity than that expected from binding studies performed with platelets (Girma et al., 1992).

We recently reported that the anti-vWF antibody 1C1E7 causes a conformational change in the vWF molecule, which is accompanied by an enhanced affinity of the high vWF multimers for GPIb (Tornai et al., 1993). In contrast with the weak effect that a control monoclonal antibody exerts, in the presence of an excess of 1C1E7, the botrocetin-mediated binding of vWF is enhanced and saturates at a higher plateau value (Figure 2c). Simultaneously performed binding studies on GPIb-coated plates pretreated with the anti-GPIb antibody AP-1 showed greatly reduced binding (Figure 2c, broken lines), in agreement with the known occupation by this antibody of the vWF-binding domain on GPIb, indicating that both binding to GPIb and the stimulation of this binding by 1C1E7 were detected specifically via the A1 loop of vWF and the N-terminal binding domain of GPIb.

Specificity of ristocetin-mediated vWF binding to GPIb

In preliminary investigations, we have shown by means of biospecific interaction analysis that ristocetin-mediated vWF binding to immobilized GPIb is a reversible event (not shown). Therefore, in view of the above analyses, coated GPIb was considered suitable for the study of ristocetin-dependent interactions between GPIb and vWF. To study this binding quantitatively, pure-GPIb-coated microtitre plates potentially offered an advantage over agglutination studies with formalin-fixed platelets, in which ristocetin-mediated interactions with other platelet proteins participate (Scott et al., 1991). Incubation of GPIb in the e.l.i.s.a. with various concentrations of both ristocetin and vWF produced saturation curves for GPIb-bound vWF similar to those previously described for the binding of vWF to particle-immobilized GPIb (Berndt et al., 1988). However, at increasing concentrations of ristocetin, non-specific vWF binding progressively predominated, as evidenced by the larger proportions of AP-1 insensitive binding (Figure 3a). The non-specific character of this binding at ristocetin concentrations exceeding 0.4 mg/ml was confirmed during incubations in plates not coated with GPIb (Figure 3b). Therefore, in order to avoid non-specific ristocetin-mediated vWF binding to coated proteins, the experimental ristocetin concentrations were limited to 0.4 mg/ml, ristocetin-dependent vWF binding to GPIb being specific below this concentration, when binding was studied in the presence of both 1C1E7 and the control antibody 7C7B3. At this concentration, ristocetin induced no flocculation of vWF, as judged from protein measurements in the centrifuged supernatant of incubation mixtures of vWF (75 μg/ml) and various concentrations of ristocetin (0–2 mg/ml). Additive effects were observed between low concentrations of ristocetin and botrocetin during vWF binding (Figure 3c). However, at 0.4 mg/ml ristocetin, the observed binding could be mainly accounted for by ristocetin,

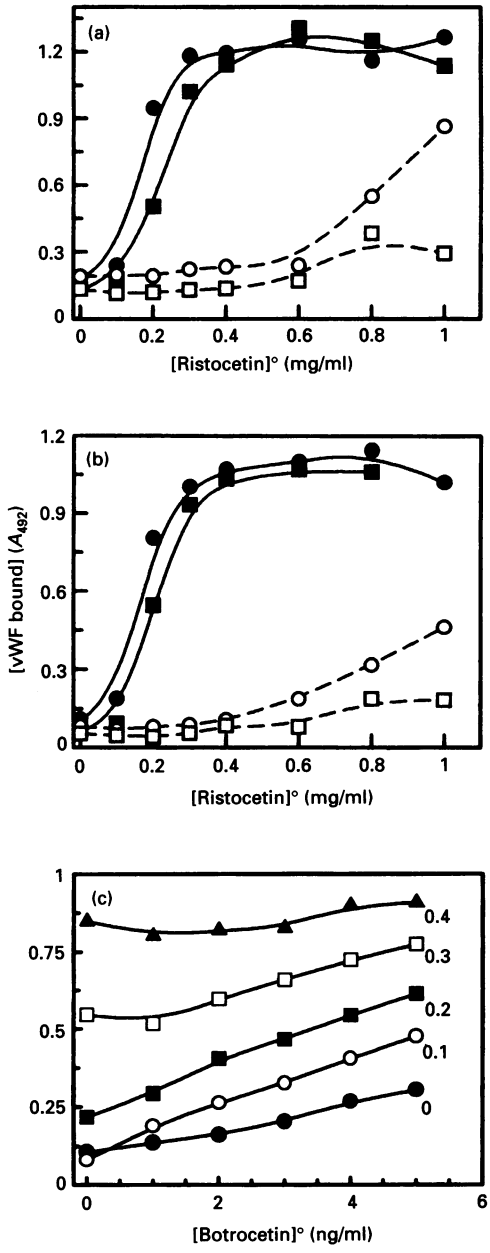

Figure 3 Specificity of ristocetin-mediated vWF binding to GPIb

(**a**) vWF (80 nM) binding to GPIb-coated microtitre plates promoted by increasing concentrations of ristocetin (0–1 mg/ml) in the presence of 50 μg/ml anti-vWF antibody 1C1E7 (●) or control antibody 7C7B3 (■). The open symbols represent the corresponding residual vWF binding to microtitre plates pretreated with the anti-GPIb antibody AP-1 at 10 μg/ml. (**b**) vWF (40 nM) binding to GPIb-coated (——) or non-coated (– – – –) microtitre plates by increasing concentrations of ristocetin (0–1 mg/ml) in the presence of 50 μg/ml anti-vWF antibody 1C1E7 (●) or control antibody 7C7B3 (■). The open symbols represent the corresponding non-specific vWF binding to the non-coated microtitre plates. (**c**) Binding of vWF (40 nM) to GPIb as a function of botrocetin concentration at the different ristocetin concentrations indicated (0–0.4 mg/ml).

suggesting that the A1-loop-mediated binding by botrocetin is diminished at higher ristocetin concentrations. Similarly, when binding in the absence or presence of an excess of antibody 1C1E7 was studied as a function of the concentration of ristocetin and vWF respectively (Figure 4), the reported effect of 1C1E7 on

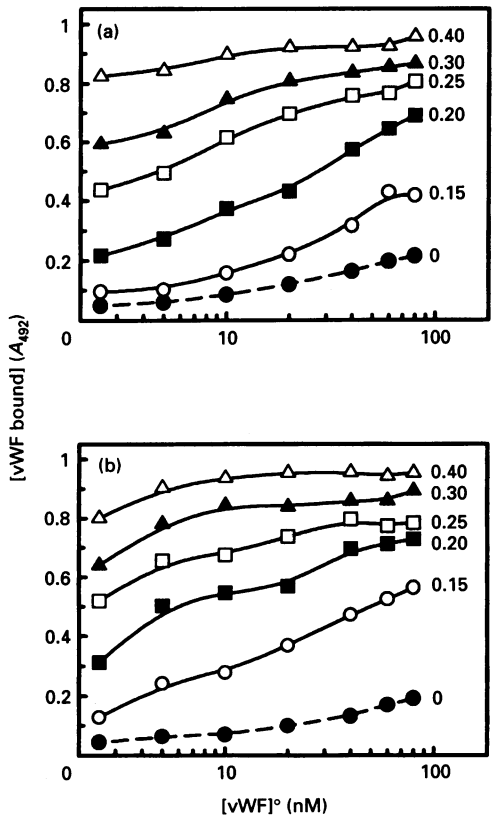

Figure 4 Ristocetin-dependent vWF A1 loop binding to GPIb

Ristocetin-mediated binding of increasing concentrations (0–80 nM) of vWF to GPIb-coated microtitre plates, measured in the absence (**a**) or presence (**b**) of an excess (50 μg/ml) of the anti-vWF antibody 1C1E7 and mediated by the ristocetin concentrations indicated (0–0.4 mg/ml).

vWF binding to GPIb could only be observed at low ristocetin concentrations, i.e. on addition of 1C1E7 a shift of the GPIb saturation curves to lower vWF concentrations could only be observed at ristocetin concentrations up to 0.25 mg/ml (Figure 4b). These experiments suggest that, above this concentration, although vWF binding is still specific (i.e. AP-1-sensitive), ristocetin induces vWF binding to GPIb independently of the binding site present on the vWF A1 loop, which is modulated by 1C1E7 (as observed both with botrocetin and at low ristocetin levels). The low degree of binding observed for high [vWF]^0 in the absence of ristocetin (Figure 4, dashed lines) was not modified by the addition of 1C1E7, indicating that this binding was non-specific and confirming that, in the absence of ristocetin, specific vWF binding to GPIb is negligible.

Mechanism of ristocetin-dependence

In order to define the importance of the A1-loop-independent interaction sites during ristocetin-mediated binding of vWF to GPIb, we analysed mechanistically the ristocetin-dependence of this binding. The valency of vWF binding to GPIb was derived from Hill plots constructed for the binding of vWF at different ristocetin concentrations in either the presence or absence of 1C1E7. As shown in Figure 5(a), for two substantially different ristocetin concentrations, parallel lines were observed with a slope equal to 0.8, revealing that, at equilibrium, the interaction of vWF with GPIb can be viewed as the binding of one vWF

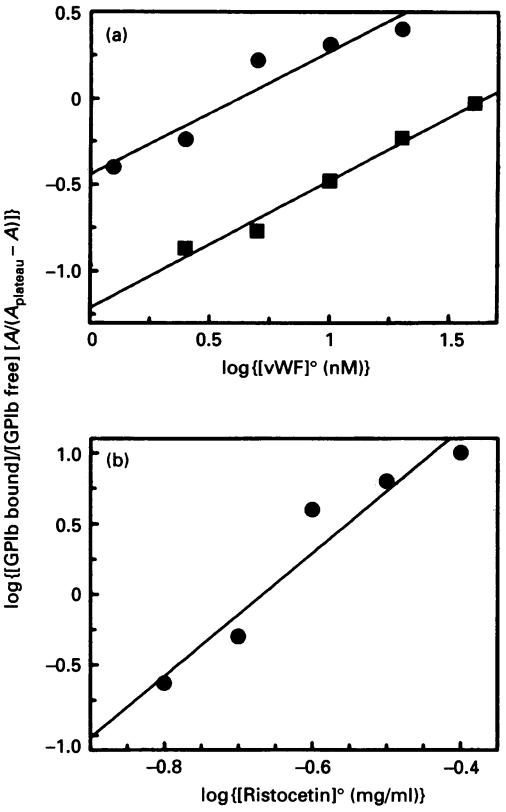

Figure 5 Stoichiometry of ristocetin-mediated vWF binding to GPIb

Hill plots for the observed e.l.i.s.a. signals during the binding of vWF to GPIb-coated microtitre plates. (**a**) Analysis with respect to $[vWF]^0$ for the binding promoted by 0.3 (●) or 0.2 (■) mg/ml ristocetin. (**b**) Analysis with respect to $[ristocetin]^0$ for binding data averaged from individual experiments performed with various vWF concentrations.

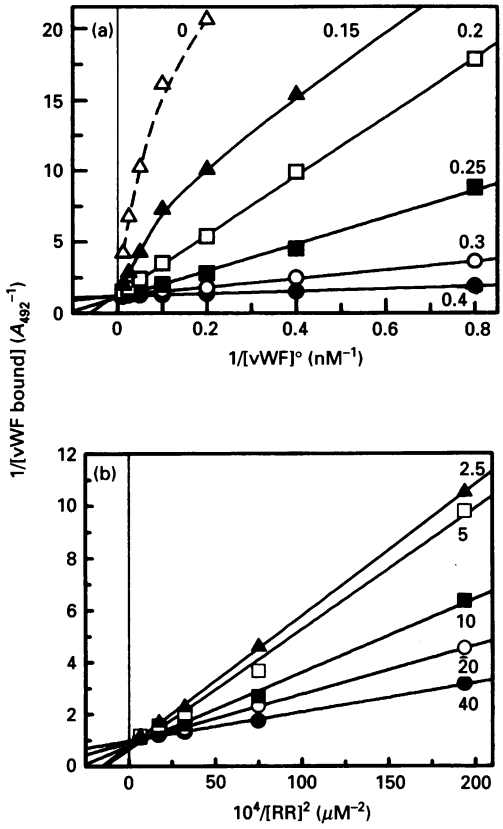

Figure 6 Mechanistic analysis of ristocetin-mediated vWF binding to GPIb

(**a**) Double-reciprocal plots of A versus $[vWF]^0$ for the binding of vWF to GPIb-coated microtitre plates mediated by the ristocetin concentrations indicated (0.2–0.4 mg/ml) and fitted curves for the binding observed in the absence (△) of ristocetin and at low ristocetin concentration (▲; 0.15 mg/ml). (**b**) Double-reciprocal plot of A versus $[RR]^2$ for the binding of vWF to GPIb-coated microtitre plates for lines constructed using the vWF concentrations indicated (2.5–40 nM).

monomer to one GPIb (1:1 stoichiometry). As outlined in the Materials and methods section, the y-intercept in this plot corresponds to $\log [RR]^2/K$. As at 0.3 mg/ml ristocetin, [RR] equals 24 μM (see below), this intersection enables us to estimate $K \approx 3 \times 10^{-18}$ M^3. Correlating the e.l.i.s.a. signals with the ristocetin concentration in Hill plots constructed for various vWF concentrations (in the absence or presence of 1C1E7) likewise revealed a slope equal to 4, indicating that the averaged specific vWF binding (i.e. AP-1-controlled) required four ristocetin molecules (Figure 5b), thus demonstrating high specificity for ristocetin in vWF binding to GPIb.

In view of the finding that the rate of vWF flocculation is limited by the involvement of two ristocetin dimers, the present findings suggest that ristocetin binds to GPIb either via interaction with four ristocetin monomers or, more probably, via binding of two ristocetin dimers (Scott et al., 1991). To confirm mechanistically the validity of Scheme 3 (which postulates a quadratic dependence on [RR] for the amount of bound vWF), [RR] values were calculated from $[R]^0$ and $K_{eq.}$ and, according to eqn. (5), double-reciprocal plots of A versus $[vWF]^0$ (at constant ristocetin concentration) and A versus $[RR]^2$ (at constant vWF concentration) were constructed. In the $1/A$ versus $1/[vWF]^0$ plot, linear relationships were observed, at least under conditions where non-specific binding of vWF to GPIb was negligible, i.e. at sufficiently low $[vWF]^0$ and high $[RR]^2$. At low ristocetin concentrations (0.15 mg/ml), no linearity was achieved in $1/A$ versus $1/[vWF]^0$ plots because under those conditions the contribution of the non-specific vWF binding (yielding non-linear double-reciprocal plots) to total vWF binding cannot be neglected (Figure 6a). Nevertheless, the regression lines constructed between 0.2 and 0.4 mg/ml ristocetin intersected on the y-axis at a single point. In agreement with the participation of two ristocetin dimers, $1/A$ versus $1/[RR]^2$ plots were linear and also intersected on the y-axis at a single point (Figure 6b). These data suggest that, at infinite $[vWF]^0$ (i.e. $1/[vWF]^0 = 0$ in Figure 6a), vWF binding does not depend on the ristocetin concentration. Likewise, at infinite $[RR]^2$ (i.e. $1/[RR]^2 = 0$ in Figure 6b), ristocetin binding does not depend on the vWF concentration. These findings imply that, in the range of ristocetin and vWF concentrations in which vWF binding to GPIb is observed, this binding does not proceed via formation of stable intermediates between ristocetin and GPIb or between ristocetin and vWF. Hence ristocetin dimers exert their stabilizing action by simultaneously interacting with both GPIb and vWF, bridging them in a quaternary complex.

Inhibition of binding by peptide polymers

In order to confirm the proposed quaternary complex-formation in ristocetin-induced vWF binding to GPIb, and to differentiate it from mechanisms in which vWF binding to GPIb would be exclusively secondary to ristocetin loading of vWF, inhibition

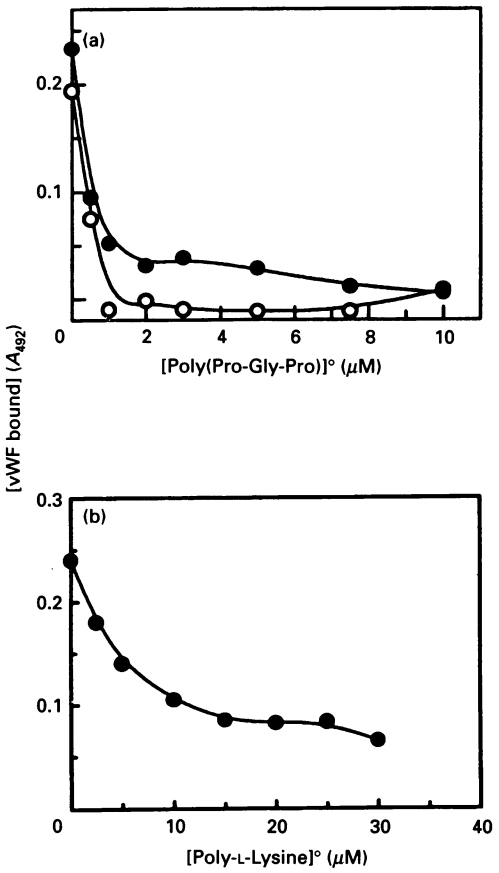

Figure 7 Inhibition of ristocetin-mediated vWF binding by polypeptides

(**a**) Inhibition of the ristocetin (0.3 mg/ml)-mediated binding of 8 nM (○) and 40 nm (●) vWF to GPIb-coated microtitre plates by increasing concentrations of poly(Pro-Gly-Pro). (**b**) Inhibition of the binding of 40 nM vWF, mediated by 0.3 mg/ml ristocetin, by increasing concentrations of poly-L-lysine.

studies were carried out with substances not expected to be inhibitory at the vWF level. Proline-rich polymers such as poly(Pro-Gly-Pro) have β-turns that complex the ristocetin dimers that are responsible for protein flocculation (Scott et al., 1991). We have confirmed that the flocculation of purified high-molecular-mass vWF multimers by ristocetin can indeed be inhibited by poly(Pro-Gly-Pro). The degree of flocculation itself was independent of the presence of 50 μg/ml 1C1E7 (not shown). As shown in Figure 7(a) for two different concentrations of vWF, specific (i.e. AP-1-sensitive) vWF binding to GPIb mediated by 0.3 mg/ml ristocetin (140 μM) was dose-dependently inhibited by poly(Pro-Gly-Pro) with an IC_{50} of 0.4 μM, i.e. at a 60-fold lower molar concentration than that calculated for the ristocetin dimers (24 μM, calculated from the equilibrium constant $K_{eq.}$ = 1.1 mg/ml = 500 μM). On the other hand, binding of vWF to GPIb has been reported to depend on the presence of negative charges in the GPIb N-terminal interaction site as well as on the presence of negatively charged *O*-glycan side chains in vWF (Carew et al., 1992). In addition, positively charged peptides were recently reported to interfere with ristocetin-mediated binding of vWF (Mohri et al., 1993). Positively charged poly-L-lysine was here confirmed to be a competitor during binding of 10 μg/ml vWF in the presence of ristocetin (0.3 mg/ml). As shown in Figure 7(b), poly-L-lysine (6–24 residues per molecule) inhibits vWF binding with an apparent IC_{50} of 10 μM; however, the specific (i.e. AP-1-sensitive) binding could not be eliminated entirely by poly-L-lysine. These findings further support the notion that the dimers of ristocetin ensure vWF binding to GPIb, not only by bridging proline-containing β-turns belonging to both proteins, but also by charge neutralization. To exclude major conformational changes in vWF as the basis of the binding mechanism, we studied the binding of asialo-vWF to GPIb in the presence of increasing ristocetin concentrations. These measurements confirmed that the spontaneously occurring interaction of asialo-vWF with GPIb was not influenced by ristocetin, unless its concentration exceeded 0.3 mg/ml (not shown). Further analysis of ristocetin (0–0.4 mg/ml)-induced vWF binding in buffers of increasing pH showed that binding was maximal at pH 7 and almost entirely eliminated at pH 8.2. Likewise, raising the ionic strength above 200 mM abolished binding entirely (not shown).

Inhibition of binding by A1-loop-flanking peptides

The very low IC_{50} found for poly(Pro-Gly-Pro) for inhibition of vWF binding suggested that this inhibitor interferes directly with ristocetin-induced vWF binding. Because, moreover, proline-rich peptides were reported to be complexed by ristocetin dimers at peptide concentrations ranging from 25 to 400 μM (Berndt et al., 1992), we have also investigated mechanistically whether the peptides Cys^{474}–Pro^{488} and Leu^{694}–Pro^{708} inhibited ristocetin-dependent vWF binding to GPIb by complexation of ristocetin dimers or by directly interfering with the formation of the quaternary complex between GPIb, vWF and RR. As expected, both the peptides Cys^{474}–Val^{489} and Leu^{694}–Asp^{709} dose-dependently inhibited ristocetin-dependent vWF binding to GPIb in the reported concentration range (Mohri et al., 1989; Berndt et al., 1992). Surprisingly though, plots of $1/A$ versus the peptide concentration yielded straight lines for both peptides, as shown in Figure 8(a) for the inhibition by peptide Leu^{694}–Asp^{709}. This plot constructed for various [RR] while maintaining the vWF concentration at 10 μg/ml (40 nM) identified a clear intersection at an apparent $K_P = 8 \pm 2$ μM, at which point the degree of vWF binding was independent of the ristocetin concentration employed. Likewise, a $1/A$ versus $[P]^0$ plot constructed for various $[vWF]^0$ while maintaining the RR concentration at 0.3 mg/ml also identified an intersection at $K_P = 16 \pm 3$ μM (Figure 8b). In agreement with the predicted proportionalities, the slope of these lines correlated with $[RR]^2$ (Figure 8a) and with $[vWF]^0$ (Figure 8b). Repeating the same analysis for the peptide Cys^{474}–Val^{489} led to the same conclusions, even though this peptide was a 2–3-fold weaker inhibitor. Double-reciprocal plots of A versus $[vWF]^0$ confirmed that the peptides behave as competitive inhibitors (Figure 8c).

Inhibition of ristocetin-induced binding by VCL

The addition of increasing concentrations of VCL to mixtures of ristocetin and vWF resulted in a dose-dependent decrease in bound vWF, at least below 125 nM VCL. At higher VCL concentrations, a dose-dependent rise in non-specific vWF binding (i.e. AP-1-insensitive) was observed (not shown), which was probably related to ristocetin-dimer-mediated complex-formation between GPIb, vWF and the progressively increasing VCL protein concentration, a phenomenon not investigated in any further detail. However, by restricting the VCL concentration to 80 nM, mechanistic analysis of its inhibitory potential was made possible. Indeed, in the concentration range 0–50 nM, VCL binding to GPIb could be detected (not shown), in parallel with the observed inhibition by VCL. Thus, in agreement with Scheme 4 and as predicted by eqn. (6), plots of $1/A$ versus $[VCL]^0$

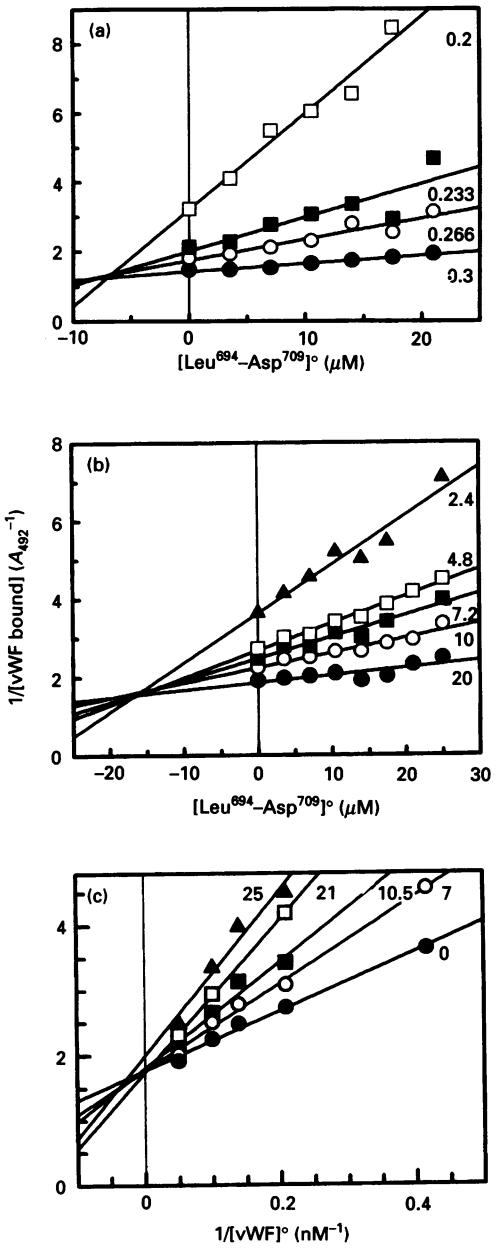

Figure 8 Inhibition of ristocetin-mediated vWF binding by Leu^{694}–Asp^{709}

(**a**) Reciprocal plots of A versus [Leu^{694}–Asp^{709}]^0, during inhibition of the binding of 40 nM vWF to GPIb-coated microtitre plates, induced by the indicated ristocetin concentrations (0.2–0.3 mg/ml). (**b**) Reciprocal plots of A versus [Leu^{694}–Asp^{709}]^0, for inhibition of ristocetin (0.3 mg/ml)-induced binding of vWF at the indicated concentrations (2.4–20 nM). (**c**) Double-reciprocal plots of A versus [vWF]^0 for the binding of vWF to GPIb-coated microtitre plates in the presence of the indicated Leu^{694}–Asp^{709} concentrations (0–25 nM) and 0.3 mg/ml ristocetin.

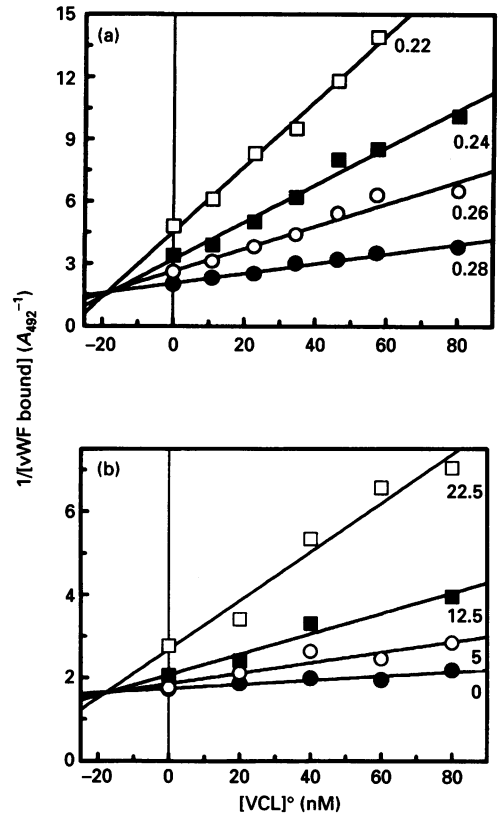

Figure 9 Inhibition of ristocetin-mediated vWF binding by VCL and by Leu^{694}–Asp^{709}

(**a**) Reciprocal plots of A versus [VCL]^0, during inhibition of the binding of 40 nM vWF to GPIb-coated microtitre plates, induced by the indicated ristocetin concentrations (0.22–0.28 mg/ml). (**b**) Reciprocal plots of A versus [VCL]^0, for inhibition of the binding of 40 nM vWF to GPIb-coated microtitre plates, induced by 0.3 mg/ml ristocetin, in the presence of the indicated Leu^{694}–Asp^{709} concentrations (0–22.5 μM).

Table 1 Summary of estimated dissociation constants for the interactions indicated

Equilibrium reaction	Experimental dissociation constant
vWF + B ⇔ vWF–B	$K_B = 0.28 \pm 0.2$ nM
GPIb + vWF–B ⇔ GPIb–vWF–B	$K_{A1} = 0.32 \pm 0.11$ nM
GPIb + VCL ⇔ GPIb–VCL	$K_{VCL} = 0.8 \pm 0.2$ nM
vWF + ATA ⇔ vWF–ATA	$K_i = 1.1 \pm 0.2$ μM
GPIb + 2RR + vWF ⇔ GPIb–$(RR)_2$–vWF	$K \approx 3 \times 10^{-18}$ M^3
GPIb + VCL ⇔ GPIb–VCL	$K'_{VCL} = 18 \pm 4$ nM*
GPIb + L^{694}–D^{709} ⇔ L^{694}–D^{709}–vWF	$K_P = 8$–16 μM*

* Values measured in the presence of ristocetin.

were linear, yielding a value for K'_{VCL} of 18 ± 4 nM (Figure 9a), reflecting a considerably weaker affinity of VCL for GPIb in the presence of ristocetin than that found during inhibition of botrocetin-mediated vWF binding to GPIb ($K_{VCL} = 0.8$ nM).

Finally, co-inhibition studies were performed involving both VCL and Leu^{694}–Asp^{709}, at constant concentrations of ristocetin and vWF, to investigate whether VCL and the peptide acted in concert but independently of each other. Under conditions in which the inhibitors act independently, an intersection is expected at [vWF]$^0 = -K'_{VCL}$, i.e. at the concentration predicted for inhibition experiments performed with VCL as the exclusive inhibitor. Indeed, during this type of complex inhibition (Figure 9b), a linear relationship was observed for $1/A$ versus [VCL]^0 plots when constructed for various concentrations of Leu^{694}–

Asp^{709}. These lines intersected at $[VCL]^0 = -16 \pm 5$ nM, a value similar to that found in studies in which VCL was the exclusive inhibitor. Thus these complex inhibition studies confirmed that VCL binding to GPIb was not influenced by the presence of peptide, i.e. VCL and the peptide inhibit vWF binding by different mechanisms.

A summary of the interactions studied, along with the estimated affinity constants derived for these equilibria, is provided in Table 1.

DISCUSSION

The vWF-binding sites for heparin, collagen, sulphatides and GPIb are all located within or in close proximity to a disulphide loop formed by Cys^{509} and Cys^{695} (Meyer and Girma, 1993). The GPIb-binding site in normal vWF is only exposed at appropriate shear stresses after vWF binding to vascular subendothelium, secondary to vessel-wall damage. In view of the fact that a large number of amino acid mutations in the A1 loop (type IIB von Willebrand disease) result in enhanced affinities of the resulting vWF mutants for GPIb (Ginsberg and Sadler, 1993), it seems plausible that minor conformational changes in the A1 loop are sufficient to promote binding of vWF to GPIb, via peptide sequences located in the A1 loop (Berndt et al., 1992). A recent report suggests that individual amino acid substitutions just outside the A1 loop also regulate A1-loop-dependent vWF binding to GPIb (Rabinowitz et al., 1993).

In vitro, the study of vWF–GPIb interactions and the amino acid residues involved is complicated by the fact that, at low shear forces, non-physiological agonists such as ristocetin and botrocetin are required to induce this interaction. In the present study we have analysed mechanistically the effect of botrocetin on the binding of vWF to GPIb, confirming that botrocetin binding to the A1 loop of vWF results in the complex acquiring a very high affinity for GPIb. The anti-vWF antibody 1C1E7 further modulated the A1-loop domain structurally, resulting in an additional increase in botrocetin–vWF affinity for GPIb and an increase in the maximum amount of vWF bound. This observation is compatible with our previous findings that the binding of the higher vWF multimers in particular to the platelet GPIb receptor is enhanced in the presence of 1C1E7 (Tornai et al., 1993). The specificity of this binding was supported by inhibition studies using VCL, an A1-loop analogue capable of directly binding with high affinity to the GPIb receptor site and thus of competing for binding with the botrocetin–vWF complex.

Ristocetin-induced vWF binding to GPIb is less well understood and has been reported to depend largely on contributions from sequences flanking the A1 loop (Mohri et al., 1989). Because monoclonal antibodies were also found to differentiate between botrocetin- and ristocetin-mediated vWF binding to GPIb (Girma et al., 1990), it has been postulated that the two mediators promote vWF binding to GPIb via different sites. Rather than searching for new sequences involved in ristocetin-mediated binding of vWF to GPIb, in the present study we have focused on the actual role ristocetin plays in promoting this binding. In order to avoid non-specific ristocetin-dependent molecular interactions, we did not use whole platelets but selected the e.l.i.s.a. configuration that had proved to be most suitable during the botrocetin-mediated vWF-binding studies. In this type of assay, at least when ristocetin concentration was restricted to 0.4 mg/ml, specific vWF binding to the natural GPIb receptor site could be established, i.e. a type of binding experimentally blocked by the anti-GPIb antibody AP-1.

In the absence of ristocetin, no specific interaction between vWF and GPIb was identified, but the vWF binding observed in the presence of low ristocetin concentrations could be modulated positively by antibody 1C1E7. We have previously reported that this antibody enhanced the affinity of vWF for platelet-associated GPIb, resulting in facilitated ristocetin-mediated platelet activation by vWF, followed by aggregation (Tornai et al., 1993). The 1C1E7-dependent conformational change in the vWF A1 loop is the result of antibody binding to a distant domain (amino acid sequence 1–272), but is sufficiently potent to enhance also the activation and aggregation of platelets induced by asialo-vWF. We can conclude from the modulation of the affinity of vWF for GPIb that, especially at low ristocetin concentrations, vWF binding is A1-loop-mediated, the specificity of this effect gradually being lost at higher ristocetin levels.

Mechanistic analysis of these observations by enzyme kinetic methods revealed the participation in the overall vWF binding to GPIb of one vWF monomer per GPIb-binding site but two ristocetin dimers (Scott et al., 1991), providing stability to the GPIb–vWF complex. It seems plausible that positively charged ristocetin dimers bind in the neighbourhood of the A1 domain where they neutralize negative charges. The negative-charge-neutralizing role of ristocetin is in agreement with earlier observations that desialylation of vWF favours its interaction with the platelet GPIb receptor site (Vermylen et al., 1973; Gralnick and Williams, 1985), although the residual sugar moieties also seem to be somehow involved in the binding process (Carew et al., 1992). Similarly, a second ristocetin dimer could interact with GPIb, this interpretation being supported by the large concentration of negative charges present on the N-terminal domain of the GPIb receptor (Murata et al., 1991). The involvement of positive charges in the ristocetin molecule during this charge neutralization is further supported by the strong dependence of the binding on the pH and ionic strength and by the fact that, on removal of the negatively charged sialic acid residues of vWF, low concentrations of ristocetin are no longer capable of modulating vWF binding to GPIb. Positively charged polypeptides such as poly-L-lysine are therefore inhibitory because they compete with positively charged ristocetin for binding to the negatively charged residues present on both proteins.

Non-specific as well as vWF-derived proline-rich peptides were also found to inhibit the binding of vWF to GPIb. Because the degree of inhibition was related to $[P]^0$ and not to $[P]^{02}$, the inhibition was not the result of complexation of free ristocetin dimers, as recently suggested (Berndt et al., 1992), but was due to competitive binding with vWF. However, in a flow chamber with blood circulating at high shear forces these peptides cannot prevent the binding of collagen-associated vWF to the platelet GPIb receptor, indicating that, in vWF, these peptides are not part of the binding site for GPIb (Gralnick et al., 1992). In agreement with this finding, our co-inhibition studies identified separate binding sites on GPIb for VCL and the peptides, despite the fact that the two inhibitors acted competitively. As these co-inhibition studies also suggested that the binding of neither VCL nor peptide to GPIb required participation of ristocetin dimers, we assume that these peptides can interact with ristocetin (monomer)-loaded GPIb and act as inhibitors by preventing the subsequent formation of ristocetin dimer bridges on proline-rich β-turns. However, firm evidence for this interpretation is lacking. Nevertheless, Scott et al. (1991) showed that ristocetin dimers promote intermolecular cross-linking by interacting with proline-rich β-turns present in the interacting proteins. In this respect, the Pro-Gly sequence found in the N-terminal domain of GPIb (Murata et al., 1991) and the proline-rich regions just outside the A1 loop are likely candidates. It has indeed been shown by site-directed mutagenesis that mutation of the sequence of three consecutive proline residues Pro^{702}–Pro^{704} to Asp^{702}–Asp^{704} or to

Arg^{702}–Arg^{704} led to a complete loss of ristocetin-mediated vWF binding to GPIb (Azuma et al., 1993); however, this finding needs to be interpreted with caution in view of the structural role played by proline residues.

The VCL fragment is a monomeric vWF fragment corresponding to Leu^{504}–Ser^{728} which strongly inhibits vWF interaction with GPIb, when mediated by both botrocetin and ristocetin (Gralnick et al., 1992). We confirmed during botrocetin-mediated vWF-binding studies that this fragment by itself bound to GPIb with high affinity. This conclusion came from the fact that an intersection was found in the $1/A$ versus $[VCL]^0$ plots. Indeed, if VCL binding to GPIb was also mediated via botrocetin, such plots would have resulted in parallel rather than intersecting lines. A similar conclusion holds for the binding of VCL in the presence of ristocetin, which would be described by parallel $1/A$ versus $[VCL]^0$ plots if VCL binding to GPIb were mediated via ristocetin. However, the apparent affinity of VCL for GPIb was considerably lower in the presence of ristocetin than in the presence of botrocetin (Figure 1b). This can only be explained if ristocetin dimer binding occurs in the negatively charged N-terminal domain of GPIb, i.e. that part of the receptor at which the VCL fragment also has to bind, but it also suggests that additional sequences in VCL are required for the inhibition of ristocetin-mediated vWF binding, in comparison with those involved in the inhibition of botrocetin-mediated vWF binding.

In conclusion, the present study examined ristocetin-induced vWF binding to GPIb by mechanistic analysis. We found that the basis of specific vWF binding to GPIb is the participation of two ristocetin dimers which bridge the two proteins as a result of both charge neutralization and interactions with proline residues in the vicinity of the natural binding sites on GPIb and the A1 domain of vWF.

We thank Dr. Kunicki, Scripps Research Institute, La Jolla, CA, U.S.A. for his generous supply of the AP-1 antibody, and Dr. Garfinkel, Bio-Technology General, Israel, for providing the VCL fragment. This work was supported by research grant 3.0030.90 from the Belgian FGWO. J.V. is the holder of the 'Dr. J. Choay Chair in Haemostasis Research'.

REFERENCES

Azuma, H., Sugimoto, M., Ruggeri, Z. M. and Ware, J. (1993) Thromb. Haemost. **69**, 192–196

Berndt, M. C., Du, X. and Booth, W. J. (1988) Biochemistry **27**, 633–640

Berndt, M. C., Ward, C. M., Booth, W. J., Castaldi, P. A., Mazurov, A. V. and Andrews, R. K. (1992) Biochemistry **31**, 11144–11151

Bolhuis, P. A., Sakariassen, K. S., Sander, H. J., Bouma, B. N. and Sixma, J. J. (1981) J. Lab. Clin. Med. **97**, 568–576

Carew, J. A., Quinn, S. M., Stoddart, J. H. and Lynch, D. C. (1992) J. Clin. Invest. **90**, 2258–2267

Coller, B. S. (1985) in Platelet Membrane Glycoproteins (George, J. N., Nurden, A. T. and Philips, D. R., eds), Plenum, New York

Fujimura, Y., Titani, K., Usami, Y., Suzuki, M., Oyama, R., Matsui, T., Fukui, H., Sugimoto, M. and Ruggeri, Z. M. (1991) Biochemistry **30**, 1957–1964

Fujimura, Y., Miyata, S., Nishida, S., Miura, S., Kaneda, M., Yoshioka, A., Fukui, H., Katayama, M., Tuddenham, E. G. D., Usami, Y. and Titani, K. (1992) Thromb. Haemost. **68**, 464–469

Ginsburg, D. and Sadler, J. E. (1993) Thromb. Haemost. **69**, 177–184

Girma, J. P., Takahashi, Y., Yoshioka, A., Diaz, J. and Meyer, D. (1990) Thromb. Haemost. **64**, 326–332

Girma, J. P., Fressinaud, E., Christophe, O., Rouault, C., Obert, B., Takanashi, Y. and Meyer, D. (1992) Thromb. Haemost. **68**, 707–713

Gralnick, H. R. and Williams, S. B. (1985) J. Clin. Invest. **75**, 19–25

Gralnick, H. R., Williams, S., McKeown, L., Kramer, W., Krutzch, H., Gorecki, M., Pinet, A. and Garfinkel, L. I. (1992) Proc. Natl. Acad. Sci. U.S.A. **89**, 7880–7884

Kalafatis, M., Takahashi, Y., Girma, J. P. and Meyer, D. (1987) Blood **70**, 1577–1583

Laemmli, U. K. (1970) Nature (London) **227**, 680–685

Light, J., Williams, C. E. and Entwistle, M. B. P. (1987) Med. Lab. Sci. **44**, 272–279

Meyer, D. and Girma, J. P. (1993) Thromb. Haemost. **70**, 99–104

Mohri, H., Fujimura, Y., Shima, M., Yoshioka, A., Houghten, R. A., Ruggeri, Z. M. and Zimmerman, T. S. (1988) J. Biol. Chem. **263**, 17901–17904

Mohri, H., Yoshioka, A., Zimmerman, T. S. and Ruggeri, Z. M. (1989) J. Biol. Chem. **264**, 7361–7367

Mohri, H., Zimmerman, T. S. and Ruggeri, Z. M. (1993) Peptides **14**, 125–129

Montgomery, R. R., Kunicki, T. J., Travis, C., Pidard, D. and Corcoran, M. (1983) J. Clin. Invest. **71**, 385–389

Murata, M., Ware, J. and Ruggeri, Z. M. (1991) J. Biol. Chem. **266**, 15474–15480

Pareti, F. I., Niiya, K., McPherson, J. M. and Ruggeri, Z. M. (1987) J. Biol. Chem. **262**, 13835–13841

Rabinowitz, I., Randi, A. M., Shindler, K. S., Tuley, E. A., Rustagi, P. K. and Sadler, J. E. (1993) J. Biol. Chem. **268**, 20497–20501

Ruggeri, Z. M. and Ware, J. (1992) Thromb. Haemost. **67**, 594–599

Ruggeri, Z. M., Zimmerman, T. S., Russell, S., Bader, R. and De Marco, L. (1992) Methods Enzymol. **215**, 263–275

Scott, J. P., Montgomery, R. R. and Retzinger, G. S. (1991) J. Biol. Chem. **266**, 8149–8155

Sugimoto, M., Mohri, H., McClintock, R. A. and Ruggeri, Z. M. (1991) J. Biol. Chem. **266**, 18172–18178

Tornai, I., Declerck, P. J., Smets, L., Arnout, J., Deckmyn, H., Caekebeke-Peerlinck, K. M. J. and Vermylen, J. (1991) Haemostasis **21**, 125–134

Tornai, I., Arnout, J., Deckmyn, H., Peerlinck, K. and Vermylen, J. (1993) J. Clin. Invest. **91**, 273–282

Vermylen, J., Donati, M. D., De Gaetano, G. and Verstraete, M. (1973) Nature (London) **244**, 167–168

Waltho, J. P. and Williams, D. H. (1989) J. Am. Chem. Soc. **111**, 2475–2480

Received 3 May 1994/24 October 1994; accepted 28 October 1994